Study of metal complexation of cardenolides with divalent metal ions by Electrospray Ionization Mass Spectrometry

Gastón E. Siless, Matias Butler, Gabriela M. Cabrera

Universidad de Buenos Aires. Facultad de Ciencias Exactas y Naturales. Departamento de Química Orgánica, Ciudad Universitaria, Pabellón II, 3º piso, C1428EHA, Buenos Aires, Argentina
CONICET- Universidad de Buenos Aires. Unidad de Microanálisis y Métodos Físicos aplicados a la Química Orgánica (UMYMFOR). Facultad de Ciencias Exactas y Naturales. Ciudad Universitaria, Pabellón II, 3º piso, C1428EHA, Buenos Aires, Argentina.

Correspondence to: Gabriela M. Cabrera, Departamento de Química Orgánica, UMYMFOR-CONICET, Facultad de Ciencias Exactas y Naturales, Universidad de Buenos Aires. Ciudad Universitaria, Buenos Aires, Argentina. E-mail: gabyc@qo.fcen.uba.ar

Abstract

Cardenolides are natural products with positive inotropic and cytotoxic activity that are able to interact with metals, although the possible role that these interactions may play in their biological activity is not known. Mixtures of the following cardenolides: digoxigenin (DgG), gitoxigenin (GxG), digitoxigenin (DxG), uzarigenin (UzG) and a butenolide, 2(5H)-furanone (Fur), with different metal cations, namely Ca^{2+}, Mg^{2+}, Cu^{2+}, Co^{2+} and Zn^{2+},were studied by Electrospray Ionization Mass Spectrometry in a Quadrupole-Time of Flight. The relative stability of the most important adducts was studied by threshold collision induced dissociation, $E_{1/2}$. Computational modeling of the observed complexes with calcium was performed using DFT B3LYP/6-31G+(d,p) level of theory.
Complexes of stoichiometry $[nM+M_E]^{2+}$, with n=4 to 6 ligands and M_E a metal cation, were observed for all studied compounds. The adducts $[4M+M_E]^{2+}$ corresponded to the most intense peaks in most of the mass spectra and showed the highest $E_{1/2}$. GxG showed a higher tendency to form complexes with low coordination numbers. Calculations showed that the carbonyl oxygen of the butenolide moiety is the most important site of coordination and allowed the proposal of different binding modes to explain the differences observed in the GxG MS spectra.
A direct relationship was observed between experimental and computational data, which allowed to predict the MS behavior of these or similar compounds. The analysis can be extrapolated to other compounds with a furanone ring, and used as an analytical tool to characterize furanone compounds, or for the differentiation of DgG and GxG.

Keywords: cardenolides, metal complexation**,** 2(5H)-furanone

Funding: This work was supported by Universidad de Buenos Aires, CONICET, ANPCYT and MinCyT.

1. Introduction

Cardenolides are a family of natural compounds which share a steroidal framework with positive inotropic activity. Cardenolide glycosides, like digoxin, have been used for more than 200 years for the treatment of cardiac failures and have not been replaced by synthetic compounds. The steroid structure of the bioactive compounds must have a *cis* configuration between rings A - B and C - D and a*trans* configuration between B and C. It must also have an unsaturated γ-lactone ring attached to the 17β position, and two hydroxy groups at 3β and 14β positions. Sugar components are not related to the activity, but influence the pharmacokinetics [1].

The mechanism of action of cardenolides is attributed to the inhibition of Na^+/K^+-ATPase, raising the level of sodium ions in cardiac myocytes, which leads to an increase in the level of calcium ions via the Na^+ /Ca^{2+} exchanger (NCX), and consequently an increase in cardiac contractile force. Recently, it was demonstrated that these compounds may activate multiple downstream signal transduction pathways that may be involved in the regulation of physiological and pathological conditions [2]. Remarkably, these compounds can also induce apoptosis and inhibit the growth of cancer cell lines at similar concentrations to those found in the plasma of patients with cardiac conditions. Several mechanisms seem to take part in these antitumor effects, and this is actually a topic of intense debate. Three compounds of this family are at this time in clinical trials [3].

The interaction between magnesium and digoxin has been studied, although from a pharmacological point of view [4]. NMR spectroscopy was used to demonstrate the formation of digoxin and digitoxin complexes with calcium ions and this complex formation was related to pharmacological aspects. These experiments showed that digoxin in a high dose increases the calcium content in the heart muscle [5].

Metal complexation in solution, followed by effective transfer of charged complexes to the gas phase by Electrospray ionization (ESI) and subsequent analysis by Mass Spectrometry (MS) has proved to be an efficient way to recognize and identify these complexes [6, 7]. Metal complexes of hydroxypyridine and pyrazine *N*-oxides [8, 9], halogenated phenylmethylidenehydrazinecarbodithioates [10], cyclosporine [11], among others, have been identified previously by this technique. The characterization and the analysis of the relative stability of the complexes may be accomplished by Density Functional Theory (DFT) calculations, and these results may be used to explain and predict the behavior of these complexes in mass spectra [8].

Nowadays it is known that metal ions may be involved in the development of several diseases [12] and metal complex formation may be associated with ionophoric properties [13].

As these cardenolides exhibit biological activities in which the transport of ions is involved, a study was conducted of the interaction of four cardenolide genins: digitoxigenin (DxG), its 5-epimer uzarigenin (UzG), digoxigenin (DgG) and its isomer gitoxigenin (GxG),with different endogenous metal (II) ions such as Mg^{2+}, Ca^{2+}, Co^{2+}, Cu^{2+} and Zn^{2+}. The goal of this study was to determine binding selectivity and affinities for each metal and the different genins, to gather insight into the possible roles of these compounds in the biological activities. The observed differences between isomers were also taken into account.

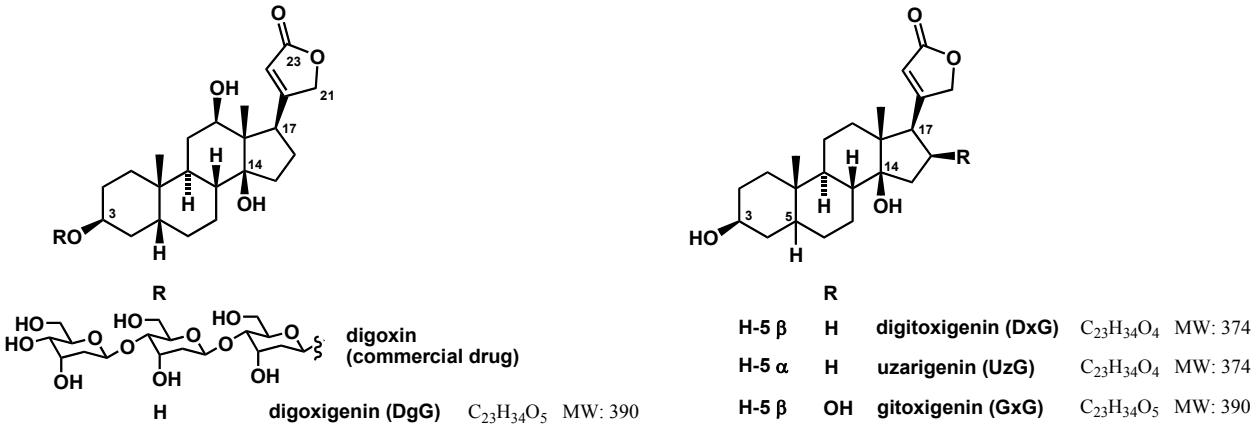

Figure 1

2. Experimental

2.1. Chemicals and reagents

The cardenolides digitoxigenin (DxG), uzarigenin (UzG), digoxigenin (DgG) and gitoxigenin (GxG), together with 2(5H)-furanone (Fur) were purchased from Sigma-Aldrich. LCMS grade methanol and HPLC grade water were purchased from Carlo Erba (Milan, Italy). The analyte solutions were prepared using methanol, each at a concentration of 10 mM. The metal ion stock solutions (10 mM) were prepared from $MgCl_2$, $CaCl_2$, $CoCl_2$, $CuSO_4$ and $ZnCl_2$ by diluting the appropriate amounts in water, as was determined in previous metal complexation studies by ESI-MS [8,9].

2.2. Instrumentation

Mass spectrometric analyses were performed using a BrukermicrOTOF-QII mass spectrometer (BrukerDaltonics, Billerica, MA, USA), equipped with an electrospray ion source. The instrument was operated at a capillary voltage of 4.5 kV with an end plate offset of -500 V, a drying gas temperature of 200 ºC using N_2 as dry gas at 4.0 L min^{-1} and a nebulizer pressure of 0.4 bar.

Multi-point mass calibration was carried out using a sodium formate solution from *m/z* 50 to 1400 in positive ion mode. Data acquisition and processing were carried out using the Bruker Compass Data Analysis version 4.0 software supplied with the instrument.

The metal solutions were added in a 2:1 ratio to the sample solutions and then infused into the mass spectrometer. Sample solutions were infused into the source using a KDS100 syringe pump (KD Scientific, Holliston, MA, USA) at a flow rate of 180 µL min^{-1}. Each experiment was repeated at least three times in different days in order to ensure reproducibility.

For CID experiments, the quadrupole mass filter was set with a 1.0 Da window for transmission (isolation) of precursor ions. Fragmentation of the mass-selected ions (CID) was performed in a collision cell with UHP Argon as collision gas. The dissociation curves were built with data from sequential CID experiments, in which the potential was incremented in 1 eV steps, starting from 6 eV up to the potential in which the precursor ion ion signal fell to zero, plus 5 eV.

The Bruker msigma algorithm, which considers the isotopic profile together with the accurate mass, was taken into account to ascertain the identity of the ions.

2.3. Computational Methods

Conformational search of $[nFur + Ca]^{2+}$ complexes (n=3-6), where Fur is 2(5H)-furanone, was performed using molecular mechanics MM+ on Hyperchem 8.0, varying the dihedral angles involving calcium and oxygen atoms. Lowest energy conformers were selected for further optimization by DFT method using Gaussian 09 [14]. Frequency calculations were performed to characterize stationary points. Geometries of neutral, singly charged and doubly charged molecules were optimized at the B3LYP hybrid density functional level of theory (DFT) [15,16] using the 6-31+G(d,p) basis set. This basis set featuring polarized orbitals proved to be well suited for the investigation of similar systems in previous studies [17,18]. The most probable coordination sites for the molecules were determined through the Gas Phase Calcium Affinity, which was calculated analogously to the Gas Phase Basicity GB [19] (Gibbs energy for the reaction $B + Ca^{2+} \rightarrow [B+Ca]^{2+}$). All the energies for protonation/complexation to Ca^{2+} were obtained by B3LYP/6–31+G(d,p). The optimized structures were characterized by harmonic frequency analysis as local minima (all frequencies real). Corrections for zero-point vibrational energy were included using the same level of theory.

All energies expressed as $\Delta H°_0$ are relative enthalpies at 0 K; those expressed as $\Delta G°_{298}$ are relative free energies at 298 K, while those expressed as ΔE (in kcal/mol) are thermal energies. Calculations were performed at the Centro de Cómputos de Alto Rendimiento (CeCAR), Facultad de Ciencias Exactas y Naturales (FCEN), Universidad de Buenos Aires.

3. Results and Discussion

The solutions containing each compound with the different metal cations were prepared just before the infusion into the mass spectrometer. The experimental conditions such as concentration of cardenolides and metal solutions, and instrumental parameters were previously determined to achieve optimal response. Some examples of the recorded spectra are shown in Figure 2. The identities of the adducts and their corresponding observed masses and relative abundances are listed in Table 1 and Tables S1-5 (Supplementary Material). The confirmation of the assignments was based on high accuracy mass-to-charge ratios, on collision induced dissociation (CID) product spectra and on the analysis of the distinctive isotopic patterns of the metals and doubly charged ions.

For all the studied compounds and metal cations, the ESI spectra showed the prevalence of signals corresponding to dicharged adducts containing from 1 to 6 cardenolide ligands. Other ligands as H_2O or MeOH were also present in the adducts, mainly when the number of steroid ligands ranged from 1 to 3. Peaks arising from singly charged adducts $[xM+M_E+Cl+yH_2O]^+$ were also observed in the spectra, being more significative for GxG and M_E=Zn (Table 1; Supplementary Tables S5).

DgG and DxG exhibited a similar behavior. Both showed signals with high relative abundance corresponding to species $[4M+M_E]^{2+}$ with all the metals, $[5M+M_E]^{2+}$ with M_E=Ca and Mg, and $[6M+Ca]^{2+}$. GxG was the cardenolide genin with the lowest affinity for metals producing a smaller number of adducts with low relative abundances as can be seen in table 1 and TS1-5 (Supplementary Material). DxG and UzG also showed peaks corresponding to $[M+H-2H_2O]^+$ with high relative abundances in almost all the spectra. The relative abundances of the signals corresponding to $[M+H-2H_2O]^+$ in the spectra obtained with the addition of metal solutions were greater than those in the spectra obtained without the addition of metals, indicating that metal coordination enhanced the fragmentation mechanisms involving the loss of water.

The ESI mass spectra with the addition of the harder Mg^{2+} and Ca^{2+} ions, which would supposedly have higher affinities for oxygen than the other metals, exhibited the presence of more peaks corresponding to adducts, and with higher relative abundance, compared to the spectra with other metals, and particularly DxG with Ca exhibited peaks with the highest relative abundances (Figure 2).

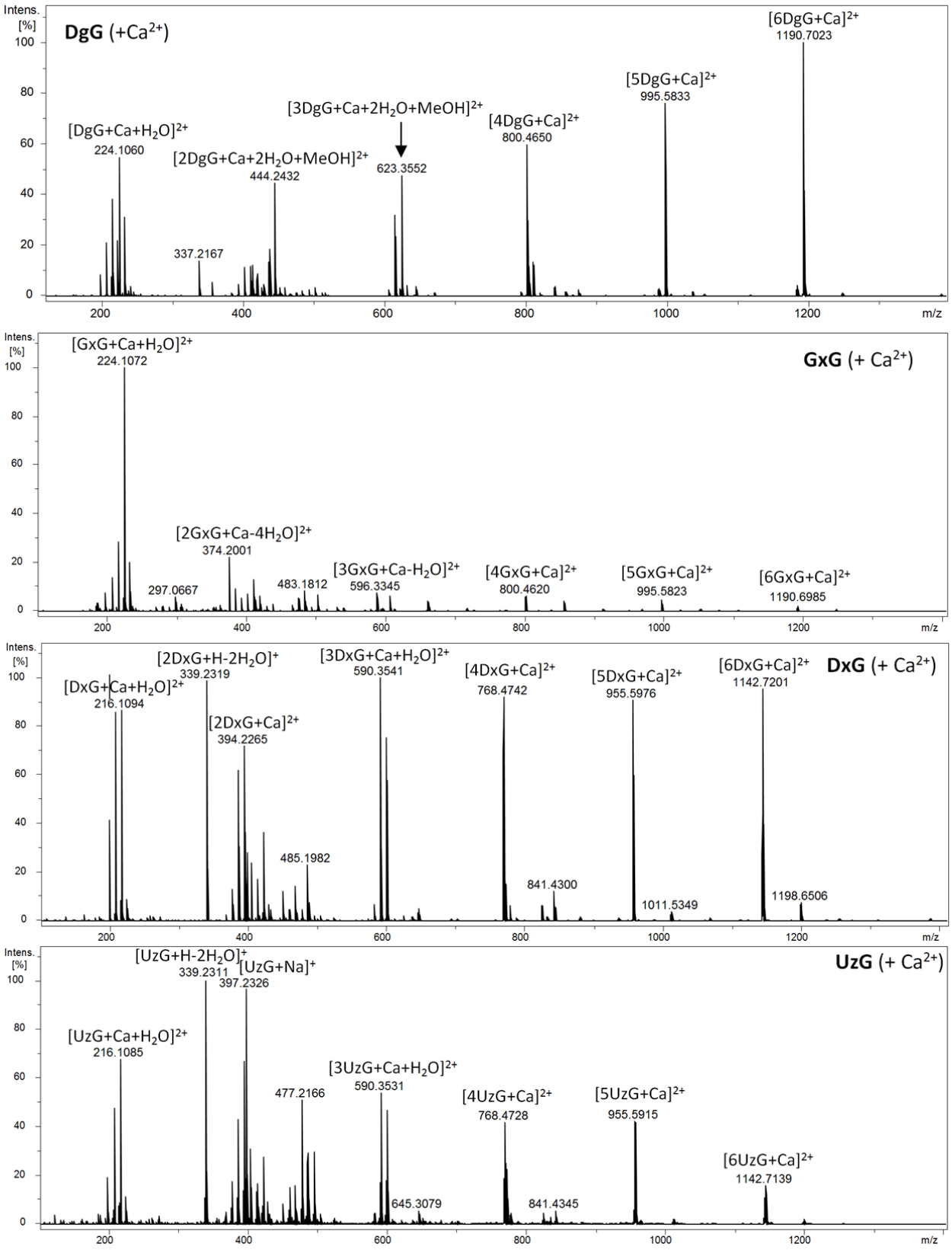

Figure 2. MS spectra of DgG, GxG, DxG and UzG with the addition of Ca^{2+} solution.

The results also indicated that the adducts of DxG and DgG with Ca^{2+}, which has an ionic radius higher than the other metals, presented higher coordination numbers up to 5 or 6, while the main coordination number was 4 for the other metal cations. A greater ionic radius may accommodate better more and larger ligands [20]. It is known that the coordination number also depends on the partial negative charge of the oxygen ligand (relatively low in the case of carbonyl oxygens) and the distance from the cation. The predominant coordination number of 4 is observed in the adducts mainly as $[4M+M_E]^{2+}$, where M is the cardenolide ligand and M_E is the metal ion, but also as other species like $[3M+M_E+H_2O]^{2+}$, particularly when M is DgG, DxG or UzG and Me is Mg, Co, Cu or Zn. Tetracoordination is usual for complexes of Co, Cu and Zn [21, 22].

In order to explore the relative stability of the adducts with different number of ligands $[nM+M_E]^{2+}$, the $E_{1/2}$ values were determined [23]. This parameter was obtained from the dissociation curves by plotting the relative abundance of the precursor ion peak as a function of the collision energy corresponding to the lab frame. The estimated $E_{1/2}$ values are summarized in Table 2 and additional information about their main fragmentation pathways are shown in table Table S6 (Supplementary Material).

As shown in Table 2, the most stable adducts were always $[4M+M_E]^{2+}$, following the order: Mg >Ca> Co > Zn > Cu. This order did not follow the same trend than the Irving-Williams series of relative complex stabilities [21,22], although it is known that inversions in the order can be possible when different conditions from high-spin octahedral complexes are not fulfilled [24].The order of stability for the cardenolide genins was DgG>DxG>UzG>GxG. For GxG, the $E_{1/2}$ of the adduct $[4M+M_E]^{2+}$ were the weakest of the genin set and were similar to those of $[M+M_E+H_2O]^{2+}$. The second stable adduct for DgG, DxG and UzG was $[3M+M_E+H_2O]^{2+}$ for all the metals except Ca, for which $[5M+Ca]^{2+}$ was the second most stable adduct. The main channels of fragmentation were the loss of a ligand for $[6M+M_E]^{2+}$ and $[5M+M_E]^{2+}$, while for the other adducts the loss of water molecules and water molecules plus cardenolide ligands were produced, via a charge separation process leading to single charged adducts.

As all the compounds have in common abutenolide ring, which can coordinate metals forming adducts with many ligands, it would be reasonable to consider that the coordination of the metals occurred *via* the butenolide moiety, and for this reason the adducts of these metals with 2(5H)-furanone (Fur), which is a simplified model of the entitled compounds, were investigated. The results are shown in table 3. In the first place, it should be noted that furanone alone is capable of coordinating all the metal cations. The favored coordination number was four in all the cases, and only with calcium a peak corresponding to $[5Fur+Ca]^{2+}$could be detected with high relative abundance. Only some small differences among the mass spectra of Fur and the cardenolides were observed. The most relevant adduct for Mg^{2+}, Co^{2+} and Zn^{2+} was $[3Fur+M_E+H_2O]^{2+}$, which yielded a fragment $[3Fur+M_E+H_2O\text{-}CO]^{2+}$, confirmed by the corresponding MS/MS spectra. The loss of CO is a known channel of fragmentation in furanones [18]. In the case of Ca^{2+} addition, the most intense peak in the mass spectrum corresponded to $[4Fur+M_E]^{2+}$, while in the case of Cu^{2+} addition, many adducts containing Cu (I) could be detected. The reduction of Cu^{2+} to Cu^{+} is a known process in ESI and it is also known that sometimes the geometry of the ligand field can influence the redox state of copper [8,21]. These results confirmed that Fur is a useful model to study the complexation of cardenolides and that the presence of a furanone ring is sufficient for metal coordination.

3.1. Geometry, coordination and energy of butenolide-Ca^{2+} complexes

The calcium gas phase affinities (Ca GPA) of the cardenolide genins were calculated in order to compare the ability of the furanone ring and the hydroxyl groups to coordinate to the divalent metal. According to this descriptor, the site of higher affinity to Ca^{2+} was the carbonyl oxygen atthe C-23 position for DgG, DxG and UzG, yielding similar values, which were approximately 25kcal/mol higher than those of the corresponding isomers coordinated *via* ahydroxyl group (Table 4). On the other hand, GxG showed a very different coordination behavior, which was in accordance with the fact that this compound also presented a distinctive mass spectrum. The Ca^{2+}cation could coordinate to the carbonyl oxygen with an angle $C_{(23)}$=O-Ca^{2+} close to 180°, through a bidentate bonding to the carbonyl oxygen at position 23 and the lactone oxygen ($O_{(21)}C_{(23)}O_{(23)}$), or *via* the hydroxyl groups 14 and 16. These results suggested that the 14, 16-*cis* diol system of GxG was able to coordinate to calcium as well or even better than the carbonyl oxygen (Supplementary Table 4 and Fig. S1). Proton gas phase basicity has been reported previously as a Ca^{2+} affinity descriptor[25], yielding a similar tendency that the calcium GPA in this case (Supplementary Table S6).

Considering the differences of Ca GPA between GxG and the other three cardenolides, the structures of the complexes $[M+Ca+H_2O]^{2+}$and $[nM+Ca]^{2+}$, with n=2-3,were also built and optimized for the four compounds. It is worth mentioning that peaks corresponding to adducts $[M+Ca+H_2O]^{2+}$ were very intense in the mass spectra of the four compounds whereas $[nM+Ca]^{2+}$, with n=2-3, were important in the spectra of DxG and UzG. The adducts $[M+Ca+H_2O]^{2+}$ converged to a bidentate configuration, in which calcium coordinated to both oxygen atoms of the butenolide and toa water molecule**.** A similar bidentate coordination was also observed for $[2M+Ca]^{2+}$, but in the case of $[3M+Ca]^{2+}$ the average bond distance between calcium and the lactone oxygen became larger, while the distance between calcium and the carbonyl oxygen became shorter, disfavoring bidentate coordination (Figure 3). Complexes with higher coordination number converged exclusively to a singly Ca^{2+}-carbonyl oxygen coordinated configuration.

Complexes $[UzG+Ca+H_2O]^{2+}$and $[DxG+Ca+H_2O]^{2+}$ with a bidentate configuration were very similar in energy, being the former only 0.2 kcal/mol higher. In a similar way, $[2UzG+Ca]^{2+}$ was 0.17 kcal/mol higher in energy than $[2DxG+Ca]^{2+}$ and $[3UzG+Ca]^{2+}$ was 0.33 kcal/mol higher than $[3DxG+Ca]^{2+}$ (Supplementary Table S8). This result is fully in accord with the similarities observed between their mass spectra (Figure 2).

On the other hand, the comparison of DgG and GxG showed some remarkable differences. Although the butenolide bidentate bonding configuration of $[M+Ca+H_2O]^{2+}$ yielded comparable energies for both compounds, the diol-bonding configuration for $[GxG+Ca+H_2O]^{2+}$ resulted 19 kcal/mol more stable than the others suggesting a higher tendency for GxG to coordinate calcium in this way[26]. The different behavior upon coordination of DgG and GxG and Ca^{2+} seemed to be a significant issue, explaining the dissimilar ESI-Ca^{2+} mass spectra of these compounds (Figure 2). It should be noted that the peak due to $[GxG+Ca+H_2O]^{2+}$ is the base peak in the corresponding mass spectrum. Moreover, the MS2 spectra of m/z 224 corresponding to $[M+Ca+H_2O]^{2+}$ for these two cardenolides, yielded completely different fragments (Supplementary Fig. S2), confirming the different nature of both adducts $[DgG+Ca+H_2O]^{2+}$ and $[GxG+Ca+H_2O]^{2+}$.

Figure 3. Calculated structures for $[UzG+Ca+H_2O]^{2+}$, $[3UzG+Ca]^{2+}$ and $[Ca(Fur)_x]^{2+}$.

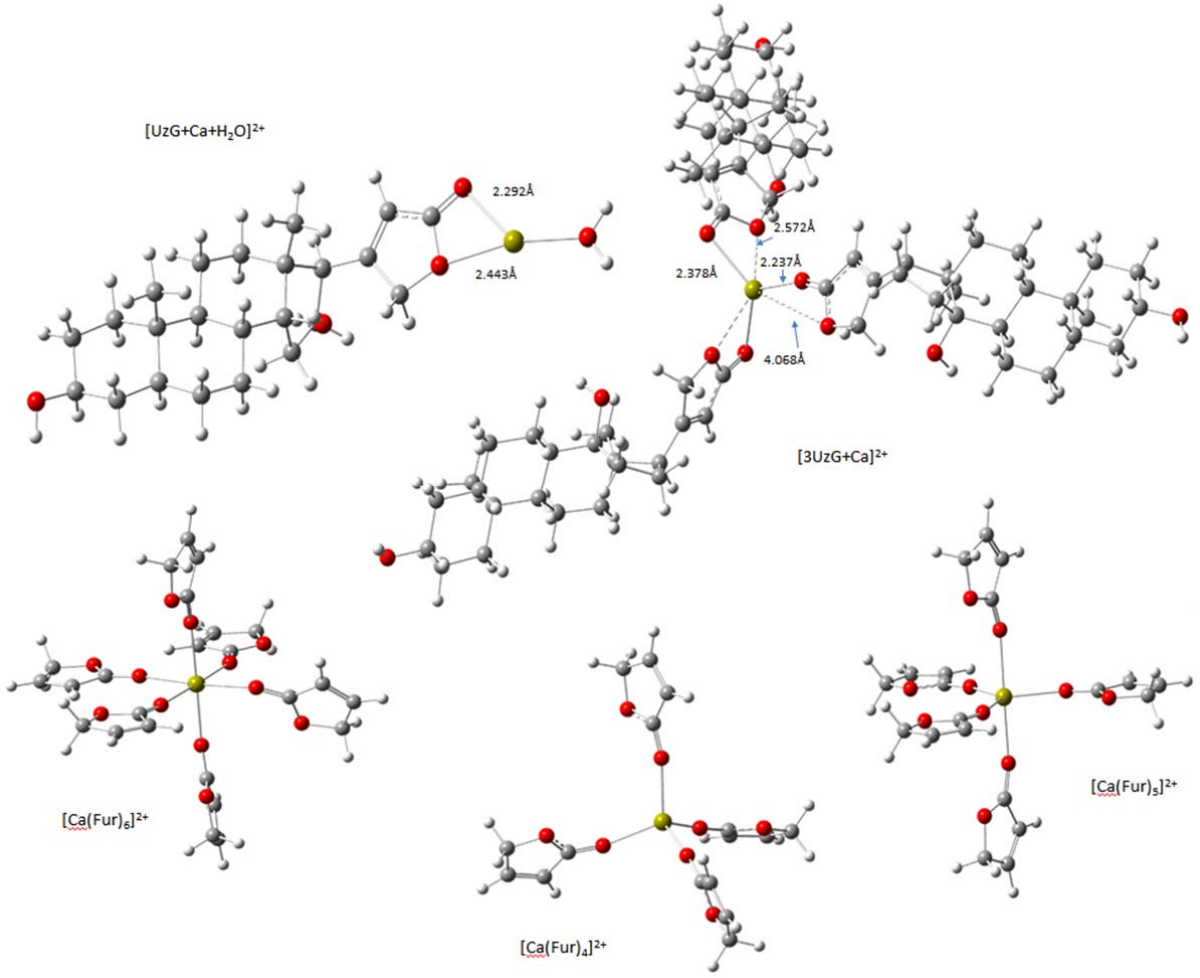

The complexes with higher coordination numbers were modeled using 2(5H)-furanone (Fur) as a simplified butenolide in order to reduce the computational cost. These complexes converged to a Ca^{2+}-carbonyl oxygen coordinated configuration, showing that the bidentate configuration is disfavored. Several conformers of Fur-Ca^{2+} complexes of low energy were inspected taking into account the higher degree of freedom of this system. The geometry around the calcium atom was in good agreement with previous reports for $Ca(H_2O)_x^{2+}$ with x=2-8 [27], yielding octahedral, trigonal bipyramidal, tetrahedral and trigonal planar structures for the $Ca(Fur)_x^{2+}$ complexes with 6, 5, 4 and 3 molecules of furanone respectively (Figure 3). The obtained average $d_{Ca\text{-}O}$ values for $Ca(Fur)_6^{2+}$, $Ca(Fur)_3^{2+}$ and $Ca(Fur)^{2+}$ of 2.37, 2.24 and 2.15 Å respectively, were also in good accord with previous reports on calcium-carbonyl complexes distances [28]. The angles for Ca-O=C system in the metal complexes were close to 170°, in contrast to the angles for H-O=C obtained for protonated molecules, which were usually around 115°. This fact may be explained by means of the higher tendency of calcium to coordinate to two lone pairs of oxygens compared with the coordination to only one hydrogen [29].

4. Summary and Conclusion

In summary, all the cardenolide steroids studied in the present work had the ability to coordinate metal cations (II) leading to many dicharged adducts differing in the number of ligands, being those with four ligands the most stable for DgG, DxG and UzG.
The complexes with calcium were modeled by B3LYP/6-31+G(d,p) showing that the calcium coordinated the compounds through the carbonyl oxygen and the lactone oxygen of the furanone ring in the adducts of low coordination number and through the carbonyl oxygen exclusively in the complexes with coordination number of four or higher. GxG was the only exception, forming also adducts with the calcium by coordination through the two *cis* hydroxyl groups at positions 14 and 16. In all the cases the calculated energies for the structure of the complexes gave a good correlation with the observed peaks in the mass spectra (those with lower energy gave peaks with higher relative abundance), indicating that the mass spectra would be predictable. Indeed, for GxG, the peak for the adduct $[GxG+Ca+H_2O]^+$ was the most intense in the mass spectrum and the structure modeled using B3LYP/6-31+G(d,p) with the calcium coordinating the hydroxyls at positions 14 and 16 was that of the minimal energy.
As the carbonyl oxygen of the furanone ring was essential for coordination, 2(5H)-furarone was also studied. The mass spectra with the addition of metal ions had similar characteristics than those of the cardenolides and the molecular modeling of the complexes, which involved a less demanding computational calculation, allowed also the interpretation of the mass spectra. In this sense, 2(5H)-furarone was a useful model for studying the reference compounds and showed that the furanone ring is the necessary and sufficient condition for coordination in the absence of other structural motifs in the molecule with this ability. Hopefully, the coordination ability can be predicted also by the above applied methodology.
The presence of different species for isomeric compounds with each metal (table 1) indicates, as an additional conclusion, that the isomeric compounds DgG vs GxG may be easily differentiated by complexation with any of the studied metals. On the contrary, DxG vs UzG showed similar spectra with most of the studied metal cations.
These results could be used to gather insights in the way that cardenolides exert their bioactivities or their secondary toxic effects at high concentrations as they would decrease the concentration and bioavailability of anycation (II) inside a cell, or may increment the metal concentration by transport. The proper mechanism of action should be further investigated. The applied methodology may be used also as an analytical tool for the differentiation of DgG and GxG or for characterization of compounds with furanone rings.

5. Acknowledgements

We thank Universidad de Buenos Aires (100352), CONICET (PIP2014-00523), ANPCYT (PICT2014-2063) and MinCyT for partial financial support.

References

[1] E. Mutschler, H. Derendorf. Drug Actions: Basic Principles and Therapeutic Aspects. Medpharm Scientific Publishers, Stuttgart(1995).
[2] I. Prassas, E. P. Diamandis, Nat. Rev. Drug Discov.7, 927 (2008).
[3] M. Slingerland, C. Cerella, H. J. Guchelaar, M. Diederich, H. Gelderblom, Invest. New Drugs. 31, 1087, (2013).
[4] G. Crippa, E. Sverzellati, M. Giorgi-Pierfranceschi, G. C. Carrara, Ann. Ital. Med. Int. 14, 40 (1999).

[5] I. S. Chekman, L. I. Budarin, N. A. Gorchakova, V. V. Tkachuk, V. N. Grebennikov, Farmakol. Toksikol. 46, 57 (1983).
[6] P. Kebarle, U. H. Verkerk, Mass Spectrom. Rev. 28, 898 (2009).
[7] V. B. Di Marco, G. G. Bombi, Mass Spectrom. Rev. 25, 347 (2006).
[8] M. Butler, P. Arroyo Mañez, G. M. Cabrera, J. Am. Soc. Mass Spectrom. 22, 545 (2011).
[9] M. Butler, G. M. Cabrera, J. Mass Spectrom. 50, 136 (2015).
[10] Y. Wu, C. Guo, N. Zhang, G. Bian, K. Jiang, Rapid Commun. Mass Spectrom. 28, 2111 (2014).
[11] R. J. Dancer, A. Jones, D. P. Fairlie, Aust. J. Chem. 48, 1835 (1995).
[12] W. Linert, H. Kozlowski (Eds). Metal Ions in Neurological Systems. Springer-Verlag, Vienna (2012).
[13] W.-Q. Ding, S. E. Lind, IUBMB Life. 61, 1013 (2009).
[14] M. J. Frisch, G. W. Trucks, H. B. Schlegel, G. E. Scuseria, M. A. Robb, J. R. Cheeseman, J. A. Montgomery Jr., T. Vreven, K. N. Kudin, J. C. Burant, J. M. Millam, S. S. Iyengar, J. Tomasi, V. Barone, B. Mennucci, M. Cossi, G. Scalmani, N. Rega, G. A. Petersson, H. Nakatsuji, M. Hada, M. Ehara, K. Toyota, R. Fukuda, J. Hasegawa, M. Ishida, T. Nakajima, Y. Honda, O. Kitao, H. Nakai, M. Klene, X. Li, J. E. Knox, H. P. HratchianHratchian, J. B. Cross, C. Adamo, J. Jaramillo, R. Gomperts, R. E. Stratmann, O. Yazyev, A. J. Austin, R. Cammi, C. Pomelli, J. W. Ochterski, P. Y. Ayala, K. Morokuma, G. A. Voth, P. Salvador, J. J. Dannenberg, V. G. Zakrzewski, S. Dapprich, A. D. Daniels, M. C. Strain, O. Farkas, D. K. Malick, A. D. Rabuck, K. Raghavachari, J. B. Foresman, J. V. Ortiz, Q. Cui, A. G. Baboul, S. Clifford, J. Cioslowski, B. B. Stefanov, G. Liu, A. Liashenko, P. Piskorz, I. Komaromi, R. L. Martin, D. J. Fox, T. Keith, M. A. Al-Laham, C. Y. Peng, A. Nanayakkara, M. Challacombe, P. M. W. Gill, B. Johnson, W. Chen, M. W. Wong, C. Gonzalez, J. A. Pople. Gaussian09. Gaussian Inc., Wallingford, CT, 2009.
[15] C. Lee, W. Yang, R. G. Parr, Phys. Rev. B. 37, 785 (1988).
[16] A. D. Becke, J. Chem. Phys. 98, 5648 (1993).
[17] I. Nicolás, M. Castro, J. Phys. Chem. A. 110, 4564 (2006).
[18] A. E. M. Crotti, E. S. Bronze-Uhle, P. G. B. D. Nascimento, P. M. Donate, S. E. Galembeck, R. Vessecchia, N. P. Lopes, J. Mass. Spectrom. 44, 1733 (2009).
[19] J.-L. M. Abboud, C. Foces-Foces, R. Notario, R. E. Trifonov, A. P. Volovodenko, V. A. Ostrovskii, I. Alkorta, J. Elguero, Eur. J. Org. Chem. 16, 3013 (2001).
[20] A. Kaufman Katz, J. P. Glusker, S. A. Beebe, C. W. Bock, J. Am. Chem. Soc. 118, 5752 (1996).
[21] K. L. Haas, K. J. Franz, Chem Rev. 109, 4921 (2009).
[22] P. W. Atkins, T. L. Overton, J. P. Rourke, M. T. Weller, F. A. Armstrong. Shriver and Atkins' Inorganic Chemistry. Fifth edition, Oxford University Press, Oxford(2010).
[23] W. M. David, J. S. Brodbelt, J. Am. Soc. Mass Spectrom. 14, 383 (2003).
[24] R. Delgado, J. J. R. Fraústo da Silva, M. Cándida, T. A. Vaz, P. Paoletti, M. Micheloni, J. Chem. Soc. Dalton Trans. 133 (1989).
[25] I. Corral, C. Trujillo, J.-Y. Salpin, M. Yañez. Ca^{2+} Reactivity in the gas phase. Bonding, catalytic effects and coulomb explosions, in Kinetics and Dynamics, from nano to bio-scale (Eds: P. Paneth A. Dybala-Defratyka) Springer, New York(2010).
[26] S. Karamat, W. M. F. Fabian, J. Phys. Chem. A. 112, 1823 (2008).
[27] R. D. Carl, P. B. Armentrout, J. Phys. Chem. A. 116, 3802 (2012).
[28] I. Corral, O. Mo, M. Yañez, A. P. Scott, L. Radom, J. Phys. Chem. A. 107, 10456 (2003).
[29] I. Corral, O. Mo, M. Yañez, J.-Y. Salpin, J. Tortajada, L. Radom, J. Phys. Chem. A. 108, 10080 (2004).

Table 1. Relative abundances of the adducts formed from DgG, GxG, DxG and UzG and Mg^{2+}, Ca^{2+}, Co^{2+}, Cu^{2+} and Zn^{2+} by ESIMS.

	DgG					GxG					DxG					UzG				
	Mg	**Ca**	**Co**	**Cu**	**Zn**	**Mg**	**Ca**	**Co**	**Cu**	**Zn**	**Mg**	**Ca**	**Co**	**Cu**	**Zn**	**Mg**	**Ca**	**Co**	**Cu**	**Zn**
$[M+H-2H_2O]^+$	1	1	1	1	2	0	0	1	3	3	1	**4**	4	2	**4**	3	**4**	4	2	**4**
$[M+H-H_2O]^+$			0	0	0			0	2	2	0		0	1	0			1		1
$[M+H]^+$	0	0	0	1	0	0		0		0	0		1	1	0	0	1	1	1	1
$[2M+H]^+$				1	0				2	0				1	0				1	0
$[M+Na]^+$	1	1	0	1	0	1	0	**4**	2	2	2	2	2	2	2	2	**4**	1	2	3
$[2M+Na]^+$	1	1	0	1	1	0	0	1	1	1	2	1	1	2	2	1	1	2	1	2
$[M+ME-H_2O]^{2+}$	1	1	1	0	1	0	1	0	4	1	1	2	0		1	1	0	1	0	0
$[M+ME]^{2+}$	2	2	2	1	2	1	2	0	1	2	1	4	0	0	1	2	2	1	0	1
$[M+ME+H_2O]^{2+}$	**4**	3	2		1	2	**4**	0		1	3	4	0		0	**4**	3	1		0
$[M+ME+2H_2O]^{2+}$							1					1					1			
$[M+ME+MeOH]^{2+}$	2	2	1		0	**4**	1				1	1	0			1	1	0		
$[M-H+ME]^+$					0										0					1
$[M-H+ME+H_2O]^+$					0										1					1
$[M+ME+Cl-2H_2O]^+$										3										
$[M+ME+Cl-H_2O]^+$										3										
$[M+ME+Cl+H_2O]^+$					1			0		2			1		1			1		2
$[M+ME+Cl+2H_2O]^+$	1	0	1		0	1	1				0	1	1		0	2	2	1		0
$[2M+ME-4H_2O]^{2+}$						2	1	1	**4**	**4**										
$[2M+ME-H_2O]^{2+}$	1	1	2	2	1	2	1	1			1	3	1	2	1	1	2	3	1	1
$[2M+ME]^{2+}$	2	1	1	0	0	1	1				2	3	1		0	2	3	1		0
$[2M+ME+H_2O]^{2+}$		1					1				1	1				3	2			
$[2M+ME+2H_2O]^{2+}$		1					0					1					1			
$[2M+ME+3H_2O]^{2+}$		1					0					2					2			
$[2M+ME+MeOH]^{2+}$	1	0	0			0					0	0				0				
$[2M+ME+MeOH+H_2O]^{2+}$	1	1			0	0					0	1					1			
$[2M+ME+MeOH+2H_2O]^{2+}$	1	2				0										0				
$[2M+ME+Cl]^+$					1					2				1				1		2
$[3M+ME-2H_2O]^{2+}$		0				1		0	1	3				0				0		
$[3M+ME]^{2+}$	0	0	0	1	0	0	1			0	1	1	1	0	1	1	0	1	0	
$[3M+ME+H_2O]^{2+}$	3	2	4	3	3	1					2	**4**	2	2	2	3	3	3	1	2
$[3M+ME+2H_2O]^{2+}$	1	2										3					2			
$[3M+ME+MeOH]^{2+}$	2	0	1		0	0					2		1					1		
$[3M+ME+Cl]^+$			1		2	0					1	0	1		1	1	0	1		
$[4M+ME]^{2+}$	4	3	**4**	**4**	**4**	1	1	0	3	2	3	**4**	**4**	**4**	4	3	2	**4**	**4**	3
$[4M+ME+H_2O]^{2+}$		1	0									1					1			0
$[5M+ME]^{2+}$	**4**	3	2	3	1	1	1	0	2	1	**4**	**4**	2	2	1	3	2	1	1	0
$[6M+ME]^{2+}$	1	**4**	1	0	0	0	0		1	0	1	**4**	0	0	0	0	1	0	0	0

0:1-5% RA; 1: 5-25% RA; 2: 25-50% RA; 3: 50-75% RA; 4: 75-100% RA. Base Peaks (or >90%) in bold. RA: relative abundance.

Table 2. E1/2 values obtained for the precursor ion signals corresponding to the different metal complexes

	E ½ (eV)																			
	Mg				Ca				Co				Cu				Zn			
precursor	DgG	GxG	DxG	UzG	DgG	GxG	DxG	UzG	DgG	GxG	DxG	UzG	DgG	GxG	DxG	UzG	DgG	GxG	DxG	UzG
$[M+ME+H_2O]^{2+}$	18.5	21.7	17.0		15.4	19.5	7.5	<6		**18.8**										
$[2M+ME]^{2+}$	11.5		6.5														15.5			
$[3M+ME]^{2+}$						8.9														
$[3M+ME+H_2O]^{2+}$	19.1	7.8	14.4	14.2					18.3	13.0	12.9	12.5	16.7	6.5	12.8	12.0	18.5		14.2	13.9
$[4M+ME]^{2+}$	**40.2**	**23.2**	**36.5**	**35.2**	**36.6**	**22.7**	**34.9**	**29.7**	**34.7**	18.5	**32.1**	**29.0**	**31.3**	**18.4**	**28.4**	**26.5**	**32.4**	**18.3**	**31.3**	**28.4**
$[5M+ME]^{2+}$	14.0		12.5	10.7	21.0	20.7	19.6	16.6	9.1	18.0	8.1	6.5	9.9	11.5	8.7	7.0	7.4	8.1	<6	
$[6M+ME]^{2+}$	8.8		6.5	<6	13.0	13.9	11.7	9.1	7.5				<6	9.3						

Table 3. Ions observed in the ESI mass spectra of 2(5H)-furanone with Mg (II), Ca (II), Co (II), Cu (II) and Zn (II); observed m/z; error in ppm; RA: relative abundances. Values in bold indicate the most abundant ion. The largest peak of the isotope distribution is given.

Me	Mg			Ca			Co			Cu			Zn		
	m/z (exp)	**err**	**RA**	**m/z** (exp)	**err**	**RA**	**m/z** (exp)	**err**	**RA**	**m/z (exp)**	**err**	**RA**	**m/z (exp)**	**err**	**RA**
$[M+H]^+$	85.0283	1.6	0.3				85.0283	1.3	3.9	85.0285	1.0	1.5	85.0286	-2.0	1.8
$[M+Na]^+$				107.0102	-1.1	1.2				107.1108	-6.8	1.2	107.0104	0.0	1.0
$[M+Na+MeOH]^+$										223.0574	1.2	14.7	223.0575	1.0	10.8
$[M+Na+2MeOH]^+$										255.0842	-1.1	23.7	255.0839	0.2	6.5
$[M+Me(I)]^+$										146.9501	0.7	89.4			
$[M+Me(I)+H_2O]^+$										**164.9613**	**-3.4**	**100**			
$[M-H+Me+H_2O]^+$													165.9526	-0.8	1.2
$[2M+Me]^{2+}$				104.0019	-0.2	1.5	113.4876	-3.7	33.5				115.9857	-4.5	12.9
$[2M+Me+H_2O]^{2+}$				113.0072	-0.1	1.8	122.4929	-3.7	38.0				124.9906	-1.2	14.8
$[2M+Me+2H_2O]^{2+}$				122.0126	-1.2	1.0	131.4986	-6.3	83.8				133.9953	3.4	34.6
$[2M+Me(I)]^+$										230.9703	4.6	64.8			
$[2M+Me(I)+H_2O]^+$										248.9818	0.2	4.0			
$[2M+Me+Cl]^+$													266.9384	4.9	25.7
$[2M+Me+Cl+H_2O]^+$	245.0078	-6.8	11.8										298.9646	4.5	12.6
$[2M+Me+Cl+MeOH+H_2O]^+$	277.0338	-5.0	4.9												
$[2M+Me+Cl+2H_2O]^+$													330.9899	6.7	13.3
$[3M+Me]^{2+}$	138.0245	-5.9	28.3	146,0129	-3.3	27.3	155.4982	-2.8	33.1	157.4966	-4.0	7.4	157.9956	0.7	45.9
$[3M+Me+H_2O\text{-}CO]^{2+}$	**133.0322**	**-5.1**	**100**				**150.5048**	**5.1**	**100**						
$[3M+Me+H_2O]^{2+}$	147.0294	-2.9	87.6	155,0184	-4.6	5.8	164.5040	-6.0	82.1	166.5011	0.7	46.5	**167.0019**	**-5.5**	**100**
$[3M+Me+2H_2O]^{2+}$							173.5088	-2.6	6.3						
$[3M+Me+MeOH]^{2+}$				162,0254	0.9	5.6							174.0079	5.1	6.4
$[3M+Me+Cl]^+$													350.9607	0.4	0.7
$[3M+Me+Cl+H_2O]^+$							279.9530	4.8	2.9						
$[3M+Me+Cl+MeOH]^+$													382.9878	-1.9	3.2
$[4M+Me]^{2+}$	180.0351	-4.7	9.4	**188.0229**	**0.3**	**100**	197.5084	-0.7	4.8	199.5072	-3.6	3.7	200.0053	4.7	7.2
$[4M+Me+H_2O]^{2+}$							206.5137	-0.8	0.7	208.5111	3.5	1.2	216.0202	-3.8	6.7
$[4M+Me+MeOH]^{2+}$				204.0357	2.1	26.1									
$[4M+Me+2MeOH]^{2+}$				220.0487	2.4	11.7									
$[5M+Me]^{2+}$				230.0342	-2.8	89.1	239.5199	-4.2	0.3				242.0175	-2.6	0.3
$[5M+Me+H_2O]^{2+}$							248.5254	-5.0	0.5						
$[5M+Me+MeOH]^{2+}$	238.0575	1.7	1.0	246.0464	1.3	45.6									
$[5M+Me+2MeOH]^{2+}$				262.0592	2.1	11.5									
$[6M+Me]^{2+}$				272.0444	-1.1	13.3	281.5299	-1.7	0.3						
$[6M+Me+MeOH]^{2+}$				288.0577	-1.5	26.5									
$[6M+Me+2MeOH]^{2+}$	296.0810	1.8	0.5	304.0714	-3.5	11.0									
$[7M+Me]^{2+}$				314.0556	-2.8	2.9	323.5405	-1.5	0.1						
$[7M+Me+MeOH]^{2+}$				330.0673	1.5	4.2									

Table 4. Ca^{2+} Gas Phase Affinities of DgG, GxG, DxG and UzG

Cardenolide	Bonding site[a]	Ca^{2+} Gas Phase Affinity (kcal/mol)	$\Delta G°_{298}rel$[c]
DgG	$C_{(23)}\mathbf{O}$	**112.73**	**1.40**
	$\mathbf{O}_{(21)}C_{(23)}\mathbf{O}_{(23)}$	**114.13**	**0.00**
	$\mathbf{O}_{(14)}$	81.47	32.65
	$\mathbf{O}_{(12)}$	89.17	24.95
	$\mathbf{O}_{(3)}$	89.23	24.90
GxG-C[b]	$C_{(23)}\mathbf{O}$	113.67	23.65
	$\mathbf{O}_{(14)}$	102.46	34.86
	$\mathbf{O}_{(16)}$	121.69	15.63
	$\mathbf{O}_{(3)}$	89.76	47.56
GxG-O[b]	$C_{(23)}\mathbf{O}$	117.23	20.09
	$\mathbf{O}_{(21)}C_{(23)}\mathbf{O}_{(23)}$	113.67	23.65
	$\mathbf{O}_{(14)}$-$\mathbf{O}_{(16)}$	**137.32**	**0.00**
	$\mathbf{O}_{(3)}$	85.67	51.65
DxG	$C_{(23)}\mathbf{O}$	112.82	1.46
	$\mathbf{O}_{(21)}C_{(23)}\mathbf{O}_{(23)}$	**114.28**	**0.00**
	$\mathbf{O}_{(14)}$	82.14	32.14
	$\mathbf{O}_{(3)}$	87.16	27.12
UzG	$C_{(23)}\mathbf{O}$	**113.74**	**0.00**
	$\mathbf{O}_{(21)}C_{(23)}\mathbf{O}_{(23)}$	**113.71**	**0.03**
	$\mathbf{O}_{(14)}$	81.76	31.98
	$\mathbf{O}_{(3)}$	85.63	28.11

a. The subscript number in parenthesis indicates the position of the atom. Atoms in bold indicates the coordination points.

b. GxG-C: Gitoxigenin conformer with hydrogen bond between OH-14 and OH-16, GxG-O: Gitoxigenin conformer without any hydrogen bond between OH-14 and OH-16.

[c] ΔG_{rel}: Calculated Free Energies relative to the lowest energy structure.